Applied Physics B (2024) 130:114
https://doi.org/10.1007/s00340-024-08250-9

Applied Physics B
Lasers and Optics

RESEARCH

Switchable multi-wavelength Pr:YLF laser based on F-P etalon

Yushi Jin[1] · Long Jin[1] · Yuan Dong[1] · Yao ma[1] · Guangyong Jin[1]

Received: 24 April 2024 / Accepted: 27 May 2024 / Published online: 6 June 2024

Abstract
We established a theoretical model of the multi-wavelength Pr:YLF laser at 604 nm, 607 nm and 639 nm based on the F-P etalon and studied the influence of the F-P etalon insertion angle on the threshold power of different wavelength lasers. The theoretical results show that by adjusting the insertion angle of a single F-P etalon, direct visible multi-wavelength laser output with different combinations can be achieved. Based on the guidance of theoretical parameters, we obtained maximum output powers of 729 mW, 420 mW, 382 mW, and 269 mW for single-wavelength at 639 nm, dual-wavelength at 604 nm&639 nm, 607 nm&639 nm, and triple-wavelength at 604 nm&607 nm&639 nm lasers, respectively, in the experiment. The experimental results agree well with the simulation. This method effectively simplifies the resonator structure and improves the conversion efficiency, providing a theoretical basis for guiding and optimizing the design of multi-wavelength laser. Such a visible multi-wavelength integrated laser source will have potential applications in fields such as laser medicine, color displays, and deep ultraviolet generation.

1 Introduction

Multi-wavelength laser in the 580–650 nm band have been widely used in various fields such as astronomy [1], laser medical treatment [2], color displays [3], and deep UV generation [4]. Especially effective in treating skin vascular diseases [5] and port wine stains [6]. The traditional method of achieving multi-wavelength laser output is obtaining multi-wavelength laser in the near-infrared band using compound resonator structures [7], followed by nonlinear frequency conversion to achieve visible multi-wavelength laser output [8, 9]. This method has disadvantages such as low system efficiency, complex optical path structure, and high cost. The orange wavelength laser obtained by organic dye lasers is widely used in laser medicine [10], but this method has the inherent drawback of the short lifetime. Pr3 + has rich transition spectra in the visible laser band, eliminating the need for second harmonic generation, and can directly output laser in the visible laser band [11, 12]. Furthermore, by modulating the transmittance loss of different wavelengths using single F-P etalon, multi-wavelength oscillation can be achieved [13, 14]. Compared to traditional methods, the F-P etalon mode selection method can not only achieve oscillation conditions between different modes based on gain control but also has advantages such as a simple structure, easy adjustment, and low cost. In 2014, Han Yang et al. were the first to use blue laser pumped Pr:YLF crystal combined with F-P etalon mode selection method to achieve multi-wavelength laser output in the visible laser band [15]. The maximum output powers of dual-wavelength laser at 604 nm&639 nm, 607 nm&639 nm, and triple-wavelength laser at 604 nm&607 nm&639 nm were 49.3 mW, 61.5 mW and 47 mW, respectively. The paper mainly describes the experimental results but doesn't carefully study the theory of F-P etalon mode selection. In 2019, Qingyu Tian et al. reported a V-shaped resonator structure Pr:YLF laser [16], which achieved simultaneous dual-wavelength laser output at 604 nm and 607 nm using a misaligned folding mirror. The dual-wavelength laser output power was 438 mW, corresponding to a conversion efficiency of 23.9%. In 2020, Xiuji Lin et al. used an output coupler with tunable transmission to obtain nearly 1W of dual-wavelength laser output at 604 nm&607 nm [17]. However, at high pump power, laser emission at 604 nm ceased due to the thermal losses, resulting in only single-wavelength laser output at 607 nm.

✉ Yuan Dong
laser_dongyuan@163.com

✉ Yao ma
mayao@cust.edu.cn

[1] Jilin Key Laboratory of Solid Laser Technology and Application, Changchun University of Science and Technology, Changchun 130022, China

This paper proposes a method of free switching of multi-wavelength laser with different wavelength combinations at 604 nm, 607 nm and 639 nm, by using only a single F-P etalon, utilizing the spectral characteristics of Pr:YLF and wavelength selection technologies of F-P etalon. This method effectively simplifies the resonator structure and improves laser conversion efficiency. In terms of theory, a theoretical model of the multi-wavelength Pr:YLF laser based on the F-P etalon is established, and the influence of the insertion angle on the threshold power of different wavelengths is studied, providing a theoretical basis for guiding and optimizing the design of direct visible multi-wavelength laser. In the experiment, guided by theoretical analysis, free switching of single-wavelength at 639 nm, dual-wavelength at 604 nm&639 nm, 607 nm&639 nm, and triple-wavelength at 604 nm&607 nm&639 nm laser were successfully achieved by simply changing the insertion angle of a single F-P etalon. The maximum output power of the triple-wavelength laser was 256 mW, with a conversion efficiency of 23.4%. The experimental results verified the accuracy of the theoretical research.

2 Model construction and simulation

The basic principle of the F-P etalon is multiple-beam interference. When multiple beams interfere with each other, the laser intensity distribution shows a regular fluctuation, selective loss is applied to different wavelengths of laser to play a role in mode selection, thereby achieving multi-wavelength laser output. The transmittance of a single F-P etalon can be expressed by the following equation [18]:

$$T(\upsilon) = \frac{1}{1 + Fsin^2(\delta/2)} = \frac{1}{1 + Fsin^2(2\pi\upsilon ndcos\theta/c)} \quad (1)$$

where F represents the finesse of the etalon, given by $F = \frac{4R}{(1-R)^2}$; R is the reflectivity of the etalon; c is the speed of light; δ is the phase difference between adjacent wavelengths in the etalon's multi-beam interference; υ represents the frequency difference between adjacent energy levels, given by $\upsilon = c/\lambda$; n is the refractive index of the etalon; d is the thickness of the etalon; θ is the angle of refraction of the beam inside the F-P etalon.

The energy level of Pr:YLF is shown in Fig. 1. The stimulated emission spectrum of the Pr:YLF crystal measured using a fluorescence spectrophotometer(Cary Eclipse, MY13450002) are shown in Fig. 2, with high peaks at 604 nm, 607 nm, and 639 nm. However, due to the higher stimulated emission cross-section at 639 nm, the 639 nm laser oscillates first, suppressing the oscillation of other wavelengths. Additionally, the 604 nm laser has high reabsorption at room temperature, making it challenging

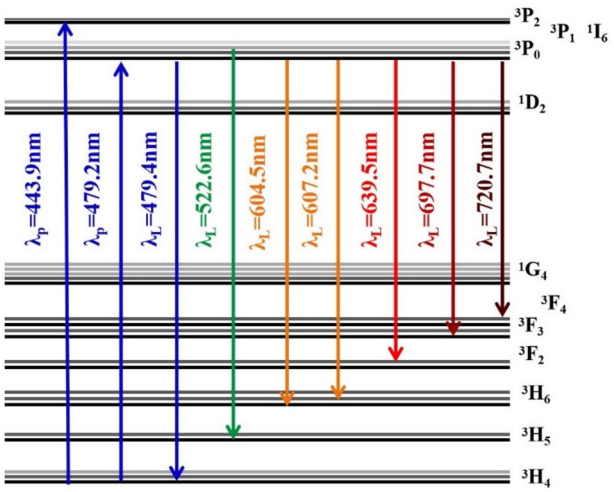

Fig. 1 The energy level of Pr:YLF

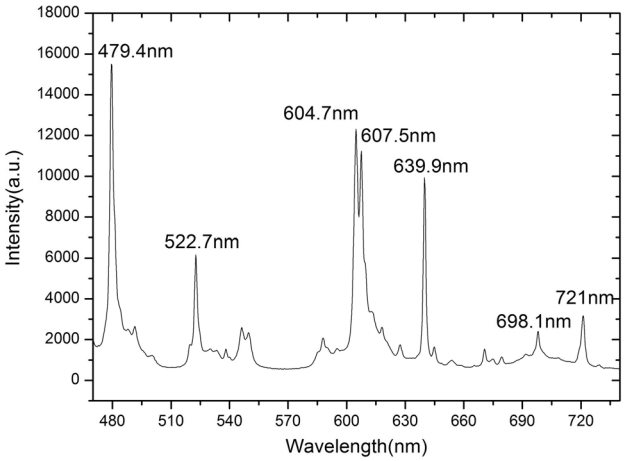

Fig. 2 Stimulated emission spectrum of the Pr:YLF crystal

to achieve laser oscillation despite having a higher emission cross-section than other wavelengths. To achieve multi-wavelength laser output, it is necessary to suppress the 639 nm laser while minimizing the losses at 604 nm and 607 nm laser. Given the proximity of the 604 nm and 607 nm wavelengths, it is not feasible to achieve mode selection through coatings of output mirror. Consequently, adjusting the F-P etalon to equalize the threshold powers of the desired wavelength emerges as a simple and effective approach for achieving multi-wavelength laser output. The specific implementation method will be discussed in the following sections.

In an ideal four-level system with spatial independence, inserting an F-P etalon is equivalent to inserting a loss, defined as $\gamma = [\gamma_i + (1 - T)]$. Then the threshold power can be expressed as:

$$P_{th} = \frac{[\gamma_i + (1-T)]}{\eta_p}\left(\frac{h\upsilon_{mp}}{\tau_f}\right)\left(\frac{A}{\sigma}\right) \quad (2)$$

Set the round-trip loss of the cavity mirror γ_i is 2%; Pump efficiency under ideal conditions $\eta_p = 1$; υ_{mp} represents the frequency difference between adjacent energy levels, given by $\upsilon_{mp} = c/\lambda i$, $\tau_f = 35.7 \times 10^{-6} s$ is the upper level lifetime, A is the area of the active medium and $A = \pi\Omega^2$, σ is the stimulated emission cross-section, The parameter data of theoretical calculation are summarized in Table 1.

The necessary condition for achieving simultaneous output of multi-wavelength laser is to equalize the threshold powers of different wavelengths, meaning that at a specific F-P etalon insertion angle, the threshold powers of multi-wavelength laser are equalized and relatively low, facilitating the generation of multi-wavelength laser outputs with greater ease. Since threshold ratios cannot simultaneously describe the threshold conditions for three different wavelengths, the threshold square difference is adopted here. Specifically, if the threshold square difference between different wavelength lasers is ≤ 0.001 W, it is considered as meeting the condition of equal thresholds. Figure 3 simulates the variation of the threshold square difference of different wavelength lasers with the F-P etalon insertion angle, along with the corresponding insertion angles and thresholds that satisfy the requirements for stable output of multi-wavelength laser.

As shown in Fig. 3, there are many F-P etalon angles that satisfy the condition of equal thresholds for different wavelengths. Due to the preference for lower thresholds and the avoidance of excessively large angle rotations of the etalon, combining these two premises can roughly determine the range of etalon angles for achieving multi-wavelength laser output. Additionally, due to the dense distribution of the angle, it is inevitable to cause the angle of multi-wavelength laser at different combinations close to each other, as indicated by the boxed angle range in the Fig. 3. The characteristic of these angle ranges is that they exhibit lower threshold powers for different combinations of multi-wavelength laser, and the differences in etalon angles varied slightly. This leads to the phenomenon of switching between different output modes, and unstable output of multi-wavelength laser. For example, when the insertion angle is around 6.5°, the threshold powers for the 604 nm&639 nm laser and the 607 nm&639 nm laser are similar, and the difference in insertion angles is less than 1°. This significantly increases the difficulty of adjusting the etalon in the experiment and affects the maximum output power due to gain competition among different wavelengths.

Considering the above factors, the optimal etalon angles selected for the dual-wavelength laser of 604 nm&639 nm, 607 nm&639 nm, and the triple-wavelength laser of 604 nm&607 nm&639 nm in the simulation are approximately 9.8°, 3.3°, and 29.4°, as indicated by the circled angle ranges in the Fig. 3. Their corresponding thresholds are 1.79W, 1.22W, and 1.65W, respectively. Next, experiments will be conducted to validate the correctness of the theoretical analysis.

3 Experiment and discussion

The experimental setup is shown in Fig. 4. The experiment utilizes a 4.2W InGaN semiconductor laser with a central wavelength of 443 nm as the pump source, with a fiber core diameter of 200 μm. The laser gain medium is an uncoated a-cut Pr:YLF crystal with a doping concentration of 5%, which has dimensions of $3 \times 3 \times 5 mm^3$ and is wrapped in indium foil and fixed in a brass heat sink. The initial water cooling temperature is set at 15 ℃.The input mirror (IM) is a plane mirror coated with an anti-reflective film at 444 nm and a high-reflectivity film in the 600–650 nm band with a reflectivity greater than 99.8%. The output coupler (OC) is a plano-concave mirror with a transmittance of approximately 5% in the 600–650 nm band as shown in Fig. 4. Considering the need to insert a Fabry–Perot (F-P) etalon into the cavity and adjust its angle, an output coupler with a curvature radius of 100 mm is selected. The etalon is fixed on a five-axis adjustment mount with a rotator, with a rotation range of ± 40° and an adjustment accuracy of 0.1°. The etalon has a thickness of 0.1 mm, a diameter of 10 mm, and is made of thin glass with no coating and high parallelism. A spectroscope (transmittance > 95% at 600–610 nm,

Table 1 Parameters of numerical simulation

Parameters (unit) -Symbol	Value	Parameters (unit) -Symbol	Value
Pumping efficiency-η_p	1	Thickness of the etalon (mm)-d	0.1
Spontaneous lifetime (μs) -τ_f	35.7	Refraction of etalon-n	1.45
0.1 mm F-P etalon reflectance-R	0.05	Round-trip loss(%)-γ_i	2
Radius of the pump beam (μs)-Ω	200	Pump wavelength (nm)-λ_{in}	444
Stimulated Sect. ($10^{-23}m^{-3}$)-σ_{604}	1	Output wavelength (nm)-λ_{604}	604
Stimulated Sect. ($10^{-23}m^{-3}$)-σ_{607}	1.41	Output wavelength (nm)-λ_{607}	607
Stimulated Sect. ($10^{-23}m^{-3}$)-σ_{639}	2.2	Output wavelength (nm)-λ_{639}	639

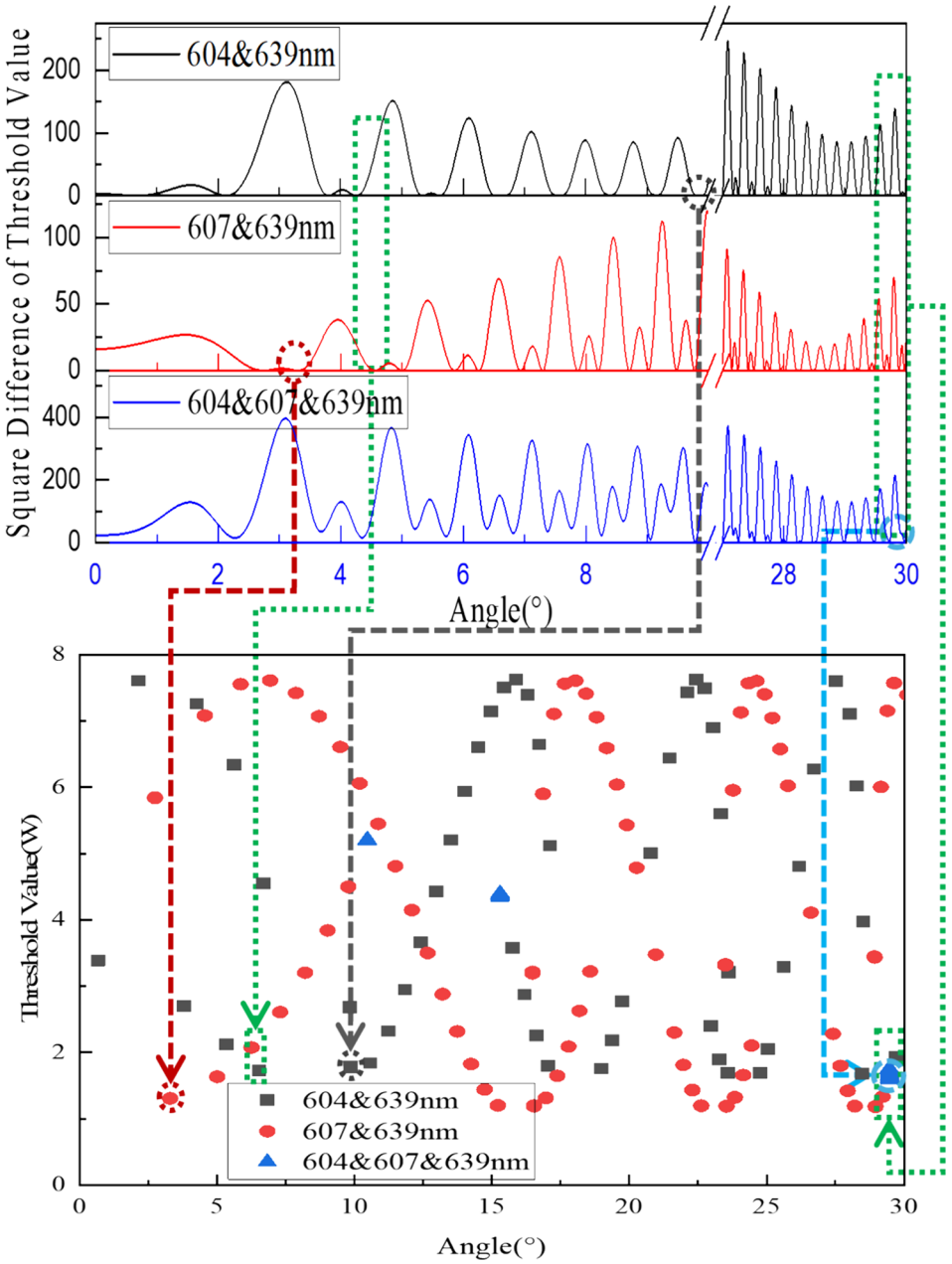

Fig. 3 The variation of the threshold square difference of different wavelength and the corresponding threshold power with the F-P etalon insertion angle

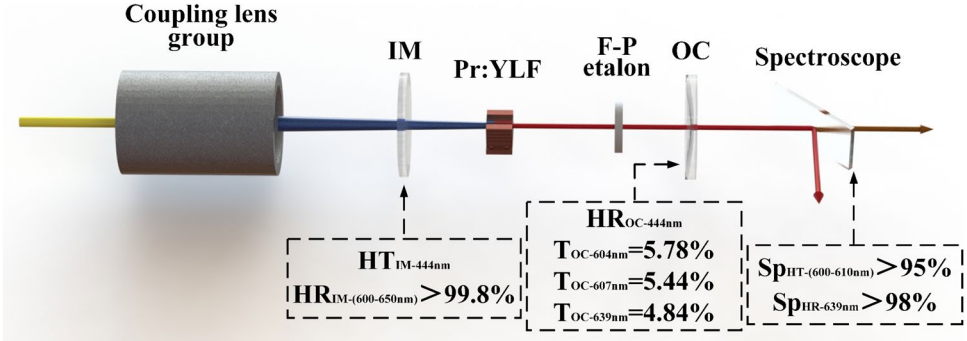

Fig. 4 The schematic diagram of the experimental setup

reflectivity > 98% at 639 nm) is placed to measure the laser beams of different wavelengths.

During the experiment, the F-P etalon is first inserted vertically to generate the 639 nm laser. Then, the cavity length and etalon position are adjusted to achieve the lowest threshold power and minimize the losses generated by the etalon. Finally, the etalon is rotated while adjusting the cavity length to achieve the highest output power for multi-wavelength operation.

Under the premise of vertically inserting the etalon, the 639 nm laser output can be achieved within the cavity length range of 49 mm to 118 mm. With an increase in crystal absorption power, the output power shows linear growth. When the cavity length is 89 mm, the highest output power of 729 mW is achieved, corresponding to a conversion efficiency of 34.4%.

Within the cavity length range of 97 mm to 112 mm, and at the maximum pump power, precise adjustment of the etalon insertion angle enables the generation of single-wavelength (639 nm), dual-wavelength, and triple-wavelength laser outputs. It was observed in the experiment that reducing the temperature of the water-cooling system makes it easier to achieve multi-wavelength laser output. This is because the energy level transitions in the orange spectral band benefit from the decrease in temperature of the active material, which reduces the losses due to reabsorption [19]. Therefore, in subsequent experiments, the water cooling temperature was set to the lowest temperature allowed by the experimental environment, which is 8 ℃.

When the cavity length is 103 cm, the highest output power for the dual-wavelength laser at 604 nm&639 nm is 420 mW, with a conversion efficiency of 30.7%. When the cavity length is 99 cm, the highest output power for the dual-wavelength laser at 607 nm&639 nm is 382 mW, as shown in Fig. 7. It can be observed that the threshold for the dual-wavelength laser at 604 nm&639 nm is lower than that for the dual-wavelength laser at 607 nm&639 nm. This differs from the simulation results, which is attributed to the significant temperature dependence of the 604 nm laser, making it easier to output at low temperatures. Additionally, when the etalon angle is around 7°, it was observed that as the pump power increases, the laser switches between single-wavelength (639 nm), dual-wavelength (607 nm&639 nm and 604 nm&639 nm) outputs. Moreover, the laser output becomes increasingly unstable with the increase in pump power, which consistent with the theoretical simulation. When the cavity length is 107 cm, the highest output power for the triple-wavelength laser at 604 nm&607 nm&639 nm is 269 mW, corresponding to a conversion efficiency of 28.5%. In the experiment, it was observed that with increasing pump power, the laser first achieves output at 639 nm, followed by dual-wavelength output at 604 nm&639 nm, and finally stabilizes at the triple-wavelength output of 604 nm&607 nm&639 nm. It should be noted that due to the small difference between the wavelengths of 604 nm and 607 nm, when the triple-wavelength laser separated by the spectroscope, only the 639 nm laser can be separated. Therefore, it is only possible to measure the combined power and spectrum of the two wavelengths in the orange spectral range. The relationship between the laser output power and crystal absorption power is shown in Fig. 8. The spectrum at the highest output power for each output mode are shown in Fig. 9. Table 2 presents the experimental data in each output mode.

Combining Figs. 5, 6, 7, 8, 9, as well as Table 2, it can be observed that the experimental results of the multi-wavelength laser align well with the theoretical simulation. The threshold power for the 639 nm laser output increases to varying degrees compared to the case of vertical insertion of the etalon. The power increase trend is also slower than before, attributed to the different angles of the etalon causing varying degrees of cavity loss. Furthermore, the output power of 639 nm laser transitions from a linear increase to a slow rise, and it gradually decreases with the increasing power of the orange spectral band laser. This is due to the intense gain competition between the 639 nm laser with a higher stimulated emission cross-section and the threshold for the 604 nm or 607 nm lasers, resulting in a decrease in the output power of the 639 nm laser.

Additionally, in the experiment of 607 nm&639 nm laser output, there is a significant discrepancy between the theoretically simulated insertion angle and the experimental angle. This is because the theoretical simulation is influenced by the 604 nm&639 nm laser under high pump power, and switching from 607 nm&639 nm laser output to 604 nm&639 nm laser output, leading to unstable laser

Table 2 Comparison of experimental data in different laser output modes

	639 nm	604 nm&639 nm dual-wavelength	607 nm&639 nm dual-wavelength	604 nm&607 nm&639 nm three-wavelength
Cavity length (mm)	89	103	99	108
Insertion angle of etalon (°)	0	10	15	30
Threshold value (mW)	429	1820	1899	2002
Output power (mW)	729	420	382	269
Conversion efficiency (%)	34.4	30.7	26.2	28.5

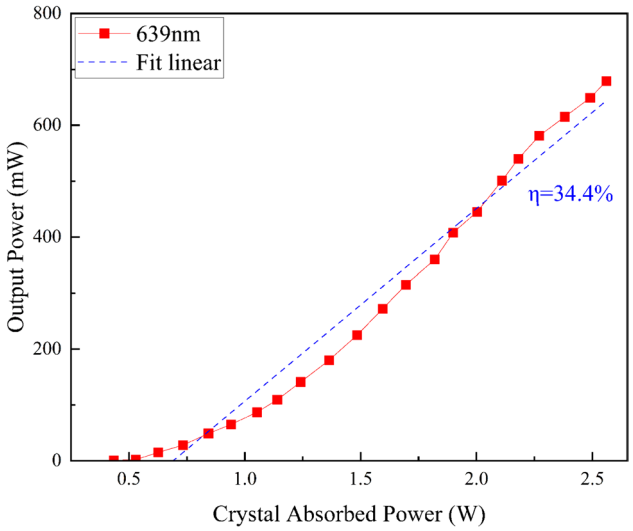

Fig. 5 639 nm laser output power versus crystal absorption power

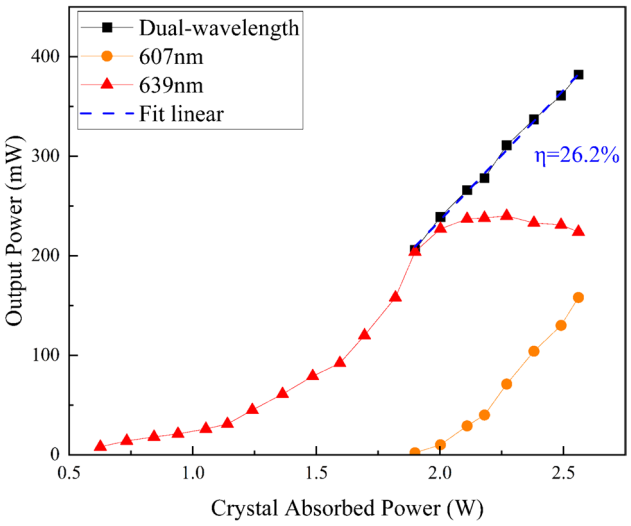

Fig. 7 Dual-wavelength (607 nm&639 nm) laser output power versus crystal absorption power

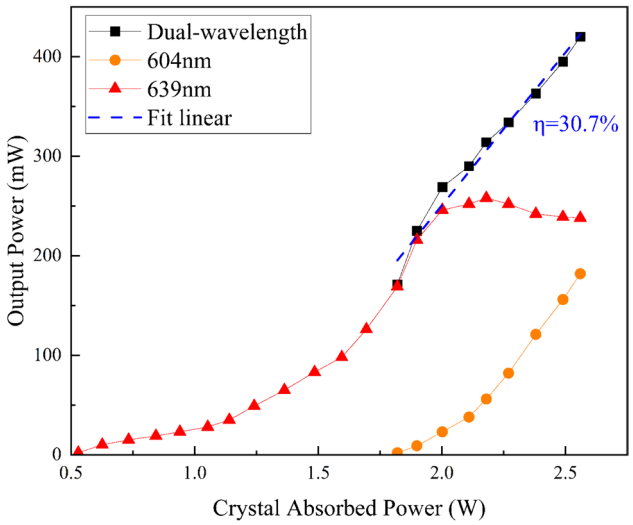

Fig. 6 Dual-wavelength (604 nm&639 nm) laser output power versus crystal absorption power

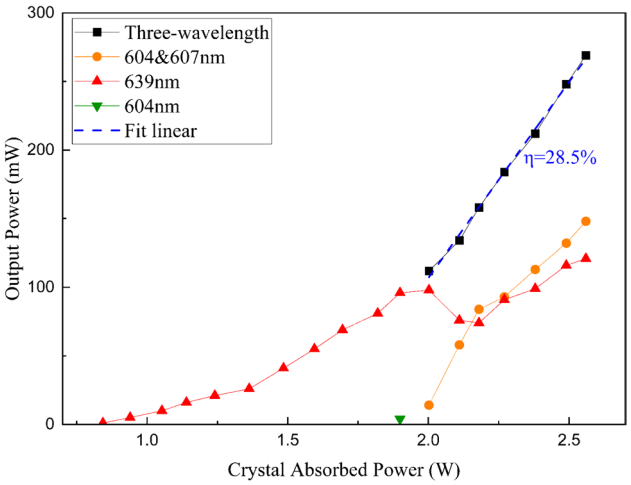

Fig. 8 Triple-wavelength laser output power versus crystal absorption power

output and lower maximum output power. When the insertion angle is 15°, the threshold for the 604 nm&639 nm laser is much higher than that of the 607 nm&639 nm laser, indicating greater losses for the former. As a result, the output of the 607 nm&639 nm laser remains stable than when the insertion angle is 3.3° (the optimal angle in theoretical simulation), which is consistent with the preference for relatively independent angles in theoretical simulation.

Stabilities of the multi-wavelength lasers have also been measured during the experiments. We recorded the maximum output power variation for half an hour in each mode, as shown in Fig. 10. At different output modes of 604 nm&639 nm, 607 nm&639 nm, and 604 nm&607 nm&639 nm, the measured fluctuations in output power (RMS) were 2.3%, 3.9%, and 2.6%, respectively. These results indicate that even under long-term working conditions, the laser output is relatively stable.

4 Conclusion

This paper innovatively proposes a theoretical model of a directly visible multi-wavelength laser based on a single F-P etalon, which enables the free switching of single and multi-wavelength (with different combinations) laser output. The theoretical model of a multi-wavelength Pr:YLF laser based on the F-P etalon is established. The impact of

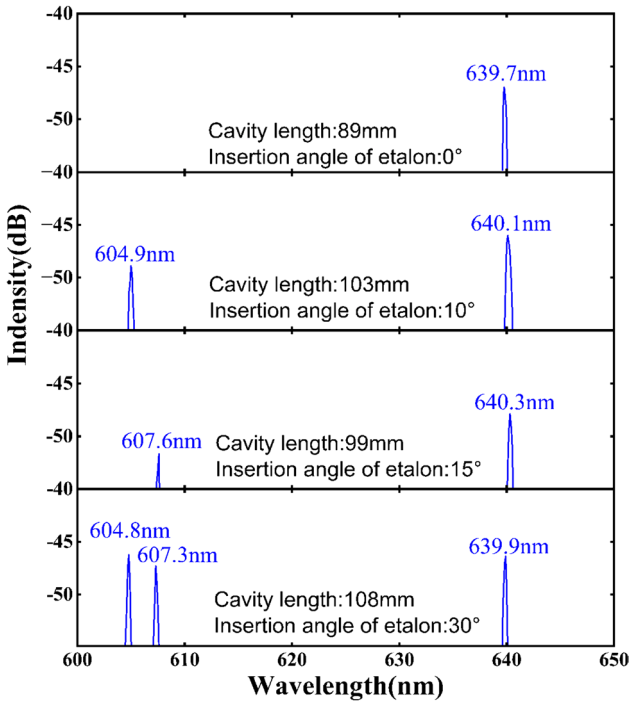

Fig. 9 The spectrum at the highest output power for each mode

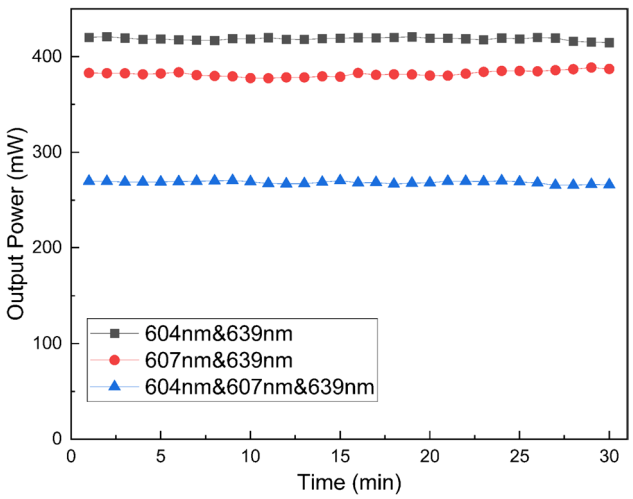

Fig. 10 Stabilities of the multi-wavelength lasers

the F-P etalon insertion angle on the threshold power of different wavelength laser is analyzed through simulations, and the experimental results align well with the theoretical simulations. Comparative experiments demonstrate that by adjusting the insertion angle of the etalon without changing any other optical elements, stable outputs of single and multi-wavelength (with different combinations) laser can be achieved. The experiment obtained maximum output powers of 729 mW for the 639 nm single-wavelength laser, 420 mW for the 604 nm&639 nm dual-wavelength laser, 382 mW for the 607 nm&639 nm dual-wavelength laser, and 269 mW for the 604 nm&607 nm&639 nm triple-wavelength laser. This theoretical model can be applied to most solid-state lasers with rich emission spectrums, providing a theoretical basis for guiding and optimizing the design of multi-wavelength lasers.

Acknowledgements We thank the Key Laboratory of Jilin Province Solid-State Laser Technology and Application for the use of the equipment.

Author contributions Yushi Jin: Writing-Original draft preparation, Writing-Review & Editing, Methodology;Long Jin: Validation, Conceptualization, Formal analysis;Yuan Dong: Project administration, Supervision;YAO MA: Software , experiment;Guangyong Jin: Resources ;

Funding This work was supported by Science and Technology Department of Jilin Province in China (Grant No. 20240402052GH).

Data availability A detailed description of the theoretical simulation has been provided, and important relevant data is included in the manuscript. The data of program are available from the corresponding author on reasonable request.

Declarations

Conflict of interest The authors declare no conflict of interest.

References

1. X. Huo, Y. Qi, Y. Zhang et al., Research development of 589 nm laser for sodium laser guide stars. Opt. Laser. Eng. **134**, 106207 (2020)
2. J. Janousek, S. Johansson, P. Tidemand-Lichtenberg et al., Efficient all solid-state continuous-wave yellow-orange light source. Opt. Express **13**(4), 1188–1192 (2005)
3. K.V. Chellappan, E. Erden, H. Urey, Laser-based displays: a review. Appl. Optics **49**(25), F79–F98 (2010)
4. S. Fujita, H. Tanaka et al., Intracavity second-harmonic pulse generation at 261 and 320 nm with a Pr3+:YLF laser Q-switched by a Co2+:MgAl2O4 spinel saturable absorber. Opt. Express **27**(26), 38134–38146 (2019)
5. M. Valdebran, B. Martin, K.M. Kelly, State-of-the-art lasers and light treatments for vascular lesions: from red faces to vascular malformations. Semin. Cutan. Med. Surg. **36**(4), 207–212 (2017)
6. J.K. Chen, P. Ghasri, G. Aguilar et al., An overview of clinical and experimental treatment modalities for port wine stains. J. Am. Acad. Dermatol **67**(2), 289–304 (2012)
7. G. Shayeganrad, L. Mashhadi, Dual-wavelength CW diode-end-pumped a-cut Nd:YVO4 laser at 1064.5 and 1085.5 nm. Appl. Phy. B **111**(2), 189–194 (2013)
8. J.L. He, J. Du, J. Sun et al., High efficiency single-and dual-wavelength Nd: GdVO4 lasers pumped by a fiber-coupled diode. Appl. Phy. B **79**, 301–304 (2004)
9. J. Liao, J.L. He, H. Liu et al., Simultaneous generation of red, green, and blue quasi-continuous-wave coherent radiation based on multiple quasi-phase-matched interactions from a single, aperiodically-poled LiTaO3. Appl. Phys. lett **82**(19), 3159–3161 (2003)

10. S.H. Woo, H.H. Ahn, S.N. Kim et al., Treatment of vascular skin lesions with the variable pulse 595 nm pulsed dye laser. Dermatol. Surg. **32**(1), 41–48 (2006)
11. P.W. Metz, F. Reichert, F. Moglia, S. Müller, C Kr¨ankel, et al., High-power red, orange, and green Pr3+:LiYF4 lasers. Opt Lett **39**(11), 3193–3196 (2014)
12. S. Luo, X. Yan, Q. Cui et al., Power scaling of blue-diode-pumped Pr:YLF lasers at 523.0, 604.1, 606.9, 639.4, 697.8 and 720.9 nm. Opt. Commun. **380**, 357–360 (2016)
13. Y.S. Zhang et al., Blue diode-pumped single-longitudinal-mode Pr:YLF lasers in orange spectral region–sciencedirect. Opt. Laser. Technol **130**, 106373 (2020)
14. Y Cheng, B Xu, B Qu, et al. "Orthogonally polarized dual-wavelength diode-pumped Pr^{3+}:$LiYF_4$ lasers at 604 and 607 nm," Advanced Solid State Lasers. Optica Publishing Group. ATh2A.15 (2014)
15. H. Yang, B. Xu, Z.P. Cai, Orange laser at 604 nm and multiwavelength emissions of orange and red laser of Pr^{3+}: $LiYF_4$ pumped by blue LD. Acta Opt Sin **34**(10), 1014003 (2014)
16. Q. Tian, B. Xu, N. Li et al., Direct generation of orthogonally polarized dual-wavelength continuous-wave and passively Q-switched vortex beam in diode-pumped Pr:YLF lasers. Opt. Lett. **44**(22), 5586 (2019)
17. X. Lin, Y. Zhu, S. Ji et al., Highly efficient LD-pumped 607 nm high-power CW Pr^{3+}:YLF lasers. Opt. Laser. Technol **129**, 106281 (2020)
18. X.M. Duan, Y. Ding, B.Q. Yao et al., A stable diffusion-bonded Tm:YLF bulk laser with high power output at a wavelength of 1889.5 nm. Chin. Phys. Lett. **31**(7), 96–98 (2014)
19. Y. Cheng, J. Peng, B. Xu et al., Passive Q-switching of Pr:$LiYF_4$ orange laser at 604 nm using topological insulators Bi2Se3 as saturable absorber. Opt. Laser Technol. **88**, 275–279 (2017)